Hardy's test versus the Clauser-Horne-Shimony-Holt test of quantum nonlocality: Fundamental and practical aspects

Daniel Braun[1,*] and Mahn-Soo Choi[2,†]
[1]*Laboratoire de Physique Théorique, Université Toulouse and CNRS, 31062 Toulouse, France*
[2]*Department of Physics, Korea University, Seoul 136-713, Korea*
(Received 31 July 2008; published 19 September 2008)

We compare two different tests of quantum nonlocality, both in theoretical terms and with respect to a possible implementation in a mesoscopic circuit: Hardy's test [L. Hardy, Phys. Rev. Lett. **68**, 2981 (1992)] and the Clauser-Horne-Shimony-Holt (CHSH) test, the latter including a recently discovered inequality relevant for experiments with three possible outcomes [D. Collins and N. Gisin, J. Phys. A **37**, 1775 (2004)]. We clarify the geometry of the correlations defined by Hardy's equations with respect to the polytope of causal correlations, and show that these equations generalize to the CHSH inequality if the slightest imperfections in the setup need to be taken into account. We propose a mesoscopic circuit consisting of two interacting Mach-Zehnder interferometers in a Hall bar system for which both Hardy's test and the CHSH test can be realized with a simple change of gate voltages, and evaluate the robustness of the two tests in the case of fluctuating experimental parameters. The proposed setup is remarkably robust and should work for fluctuations of beam splitter angles or phases up to the order of 1 radian, or single particle loss rates up to about 15%.

DOI: 10.1103/PhysRevA.78.032114 PACS number(s): 03.65.Ud, 03.67.−a, 73.23.−b, 73.43.−f

I. INTRODUCTION

The belief that nature should be describable by a local realistic theory is deeply rooted in our classical intuition [1]. Impressive evidence has been accumulated to the contrary, however, starting with the pioneering work by Bell [2]. He showed that the assumptions of locality and reality lead, in the framework of classical probability theory, to bounds on the correlations of measurement outcomes of spatially separated observers. Experiments with entangled photons have shown that the quantum world does not obey these bounds [3]. Violations of Bell's inequality by tens of standard deviations have been observed meanwhile, while being in excellent agreement with the quantum mechanical predictions [4]. Such quantum correlations have become known as "quantum nonlocality." Several proposals have been put forward to observe entanglement [5–10] or even a violation of Bell's inequality in mesoscopic circuits [11,12]. None of these has been implemented experimentally so far, even though the two-particle Aharonov-Bohm effect [7] demonstrated in a recent experiment [13] suggests the presence of the electron entanglement. On the other hand, a violation of a modified Bell's inequality has been observed in a circuit-QED system very recently [14]. From a foundational perspective, it is desirable to observe a violation of a Bell inequality in a material system, as one of the key requirements for a conclusive refutation of any local hidden variable (LHV) description of an experiment is the knowledge of the pair production rate. As was shown by Santos, a LHV description is always possible if the probabilities are obtained as relative frequencies normalized to (the sum of) joint-coincidence rates rather than to absolute pair production rates, even in the case of ideal polarizers and detectors [15]. This requirement is hard to meet in quantum optical experiments, but should be feasible with material particles, which are easier to keep track of than photons. Progress was recently achieved in this direction in an experiment with trapped ions [16].

In this paper we compare two different kinds of tests of quantum nonlocality and their mutual relations: Hardy's test [17,18] and the Clauser-Horne-Shimony-Holt (CHSH) test [19] (the Bell-type test based on the CHSH inequality). We compare these tests both on a purely theoretical level, and in relation to a possible experimental realization using a specific setup in a mesoscopic circuit, paying particular attention to the range of parameters in which these tests are expected to signal violation of noncontextual realism, a generalization of local realism (see below). The motivation for the first part lies in the fact that Hardy's test, which is one of the tests of "nonlocality without inequalities," has always stood apart from other tests by its simplicity and apparent reliance on pure logic. Mermin has called it "the best version of Bell's theorem" [20]. On the other hand, the CHSH inequality is special among all Bell-type inequalities: It is known to be the only relevant Bell-type inequality (for bipartite experiments with two observables per observer with two possible outcomes each) in the sense that a CHSH inequality is always violated if any other Bell-type inequality is violated (but not necessarily the other way around) [21–25]. The question then arises, what role Hardy's test plays in this context. We discuss the relation between Hardy's test and the CHSH test both in the absence and presence of imperfections. In the former case, we study the relation between the two tests in geometrical terms, making obvious the connection between the convex sets of joint probabilities of different measurements involved, while the latter is examined by means of set-theoretical arguments [26–28]. We then propose a mesoscopic circuit which allows one to implement both Hardy's test and the CHSH test by a simple change of parameters. This makes it possible to compare the two tests on an equal footing concerning the range of parameter fluctuations

*braun@irsamc.ups-tlse.fr
†choims@korea.ac.kr

which, according to quantum mechanics (QM), would still allow a refutation of noncontextual hidden variable theories.

II. HARDY'S TEST VERSUS THE CHSH TEST

A. Local hidden variable theories

As pioneered by Bell [2,29], the nonlocality of the quantum world can be tested by attempting to construct a local hidden variable theory that reproduces all quantum mechanical predictions. Such an approach leads to necessary conditions for LHV theories in the form of bounds on the correlations, the famous Bell inequalities. If in an experiment a violation of such an inequality is observed, a LHV description is ruled out and the nonlocality of the quantum world is established.

Let us consider a possible local hidden-variable description of a bipartite system. LHV models are defined by the joint probabilities $P(m_1,m_2|M_1,M_2)$ to obtain a pair of outcomes m_1 and m_2 for the observables M_1 and M_2 on "particle" 1 and 2, respectively. There can be n_1 (n_2) observables and k_1 (k_2) outcomes per observable on the side of "particle" 1 (2). We suppose that the particle 1 (2) is possessed by Alice (Bob).

There are overall $d=n_1n_2k_1k_2$ possible joint probabilities, but they are not all independent and have to satisfy several constraints. First of all, all joint probabilities must be nonnegative and normalized, such that for any measurement setting (M_1,M_2)

$$\sum_{m_1,m_2} P(m_1,m_2|M_1,M_2)=1. \tag{1}$$

This implies that

$$0\leqslant P(m_1,m_2|M_1,M_2)\leqslant 1 \tag{2}$$

for all m_1,m_2,M_1,M_2. Secondly, the joint probabilities must respect the causality constraint (also called nonsignaling constraint). This means that the reduced probabilities on either side must not depend on the measurement settings on the other side—otherwise superluminal signaling would be possible over sufficiently large distances:

$$\sum_{m_2} P(m_1,m_2|M_1,M_2) = \sum_{m_2'} P(m_1,m_2'|M_1,M_2') \quad \forall\ m_1,M_1,M_2,M_2', \tag{3a}$$

$$\sum_{m_1} P(m_1,m_2|M_1,M_2) = \sum_{m_1'} P(m_1',m_2|M_1',M_2) \quad \forall\ m_2,M_2,M_1,M_1'. \tag{3b}$$

Bell-type correlations are further constrained by the request of locality for each value of the hidden variables λ. In a LHV theory, the outcome of *any single run* must be, for both observers, a function of the hidden variables λ and the local measurement setting alone, such that the joint probabilities are given by

$$P(m_1,m_2|M_1,M_2)=\sum_{\lambda} p_\lambda P_\lambda^{(1)}(m_1|M_1)P_\lambda^{(2)}(m_2|M_2), \tag{4}$$

where p_λ is the normalized distribution of hidden variables, and $P_\lambda^{(j)}(m_j|M_j)$ is the probability for a given hidden variable λ that the measurement result is m_j if an observable M_j of particle j $(j=1,2)$ is measured. We have written down the locality constraint for a stochastic hidden variable theory. A deterministic HV theory is a special case, where all probabilities $P_\lambda^{(1)}(m_1|M_1)$ and $P_\lambda^{(2)}(m_2|M_2)$ are either zero or one. On the other hand, any stochastic HV theory can be made deterministic [21–23]. Note that the causality constraint above works on the level of the actually observed probabilities (i.e., for averages over hidden variables), whereas the locality constraint (4) is based on the request of nonsignaling for each value of the hidden variables.

B. Ideal Hardy's test

In 1992, Hardy proposed an experiment, which allows to test whether Nature can be described by a local realistic theory [17]. The experiment can be based on any pair of observables $M_1=X_1,Y_1$ and $M_2=X_2,Y_2$ with two mutually exclusive outcomes (which we will take as ± 1 for concreteness) for each observable. Alice (Bob) has the free choice to measure either X_1 or Y_1 (X_2 or Y_2) in any run of the experiment. The measurements of Alice and Bob should be spacelike separated, such that the measurement settings of Alice will, if one accepts Einstein locality, not influence the outcomes of Bob's experiment and vice versa. The situation first analyzed by Hardy [17] assumes three vanishing joint probabilities,

$$P(+,+|X_1,X_2)=0, \tag{5}$$

$$P(+,-|Y_1,X_2)=0, \tag{6}$$

$$P(-,+|X_1,Y_2)=0. \tag{7}$$

Suppose an experimental setup can be found where these three equations are fulfilled. Then, if Nature can be described by a LHV theory, it follows immediately that also

$$P(+,+|Y_1,Y_2)=0 \tag{8}$$

must be satisfied. In the following we will call Eqs. (5)–(8) "Hardy's equations." To see how a violation of Eq. (8) under given assumptions (5)–(7) implies nonlocality, suppose that an event with $y_1=y_2=+1$ was detected for the simultaneous measurement of Y_1 and Y_2. It follows from Eq. (6) that on Bob's side the outcome x_2 of the measurement of X_2 must have had the value +1, as $y_1=1$ can never appear with $x_2=-1$, and $x_2=+1$ is the only alternative. Similarly, from Eq. (7) follows that x_1 must have had the value +1, as $y_2=1$ can never appear with $x_1=-1$, and $x_1=+1$ is the only alternative. Furthermore, due to the locality assumption, the value of x_2 cannot depend on whether Alice measured x_1 or y_1, and x_1 cannot depend on whether Bob measured x_2 or y_2. So one concludes in a LHV theory that *both* x_1 and x_2 must have had the values +1. This, however, is excluded by Eq. (5). As a consequence, if Eqs. (5)–(7) are fulfilled, even a single event

$y_1=y_2=+1$ amidst any finite series of measurements rules out that the experiment can be described by a local realistic theory.

Hardy managed to construct a pure state for which, according to QM, just this happens [17]. Later, his argument was generalized and it was shown that almost any pure state of any system with an arbitrary number of particles and arbitrary dimension of Hilbert space can be used [30–32], and even a large class of mixed states [26].

It is instructive to determine how strongly Eq. (8) can be violated according to QM. Following Ref. [31], suppose a pure state $|\psi\rangle=b|01\rangle+c|10\rangle+d|11\rangle$ is prepared (normalized to $|b|^2+|c|^2+|d|^2=1$), where, e.g., $|01\rangle=|0\rangle\otimes|1\rangle$, the first state belongs to Alice, the second to Bob, and $|0\rangle$ and $|1\rangle$ are orthogonal basis states, which we will take as computational basis. In fact, any pure two-qubit state which is neither a product state nor a maximally entangled state can be brought to this form through an appropriate choice of orthogonal basis states [31]. Assume furthermore that the measurement operators on Alice's side are defined by $X_1=|0\rangle\langle 0|-|1\rangle\langle 1|$ and $Y_1=|y_1^+\rangle\langle y_1^+|-|y_1^-\rangle\langle y_1^-|$, where

$$|y_1^+\rangle=\frac{d^*|0\rangle-b^*|1\rangle}{\sqrt{|b|^2+|d|^2}} \tag{9}$$

and

$$|y_1^-\rangle=\frac{b|0\rangle+d|1\rangle}{\sqrt{|b|^2+|d|^2}}. \tag{10}$$

The possible measurement outcomes are obviously ± 1 for both measurements. Similarly, for Bob we define $X_2=|0\rangle\langle 0|-|1\rangle\langle 1|$ and $Y_2=|y_1^+\rangle\langle y_2^+|-|y_2^-\rangle\langle y_2^-|$, where

$$|y_2^+\rangle=\frac{d^*|0\rangle-c^*|1\rangle}{\sqrt{|c|^2+|d|^2}} \tag{11}$$

and

$$|y_2^-\rangle=\frac{c|0\rangle+d|1\rangle}{\sqrt{|c|^2+|d|^2}}. \tag{12}$$

It is then straightforward to verify [31] that Eqs. (5)–(7) are fulfilled, whereas

$$P(++|YY)=\frac{|bcd|^2}{(|b|^2+|d|^2)(|c|^2+|d|^2)}\neq 0, \tag{13}$$

where we have omitted the particle indices 1 and 2 (hereafter we will adopt this convention unless there is a risk of confusion). The joint probability $P(++|YY)$ is maximized for $|b|=|c|$ and $|d|=\sqrt{5}-2$, in which case

$$P(++|YY)=\frac{5\sqrt{5}-11}{2}\simeq 0.090\,17. \tag{14}$$

Thus, about 9% of the experimental outcomes should falsify any LHV theory, and this is the largest possible value [31]. We call such an optimized state

$$|\psi\rangle=\sqrt{2(\sqrt{5}-2)}(|01\rangle+|10\rangle)+(\sqrt{5}-2)|11\rangle \tag{15}$$

an "ideal Hardy state."

"Hardy nonlocality" has so far stood apart from other tests of local realistic theories in several aspects. First, it does not rely on inequalities, but apparently on pure logic. In the ideal setting proposed by Hardy, a single measurement event can invalidate all LHV theories. Note that for three particles such tests are known and can be based, e.g., on the Greenberger-Horne-Zeilinger (GHZ) state [33]. Secondly, Hardy nonlocality does *not* work for maximally entangled states, in contrast to the standard Bell's inequality. It is well known that the CHSH inequality [19] is maximally violated for a singlet state (and appropriately chosen measurements). It may be for these reasons that Hardy nonlocality has been called "the best version of Bell's theorem" [20]. Substantial efforts have been spent to observe Hardy nonlocality experimentally. An experiment with photons was performed by Irvine *et al.* [34] using the bunching of photons at a beam splitter (BS) in order to create a Hardy state, and by Di Giuseppe *et al.* using polarized photons in a nonmaximally entangled state [35].

C. The geometry of Hardy's test

Above we have seen several apparent differences between Hardy's test and the CHSH test. But what is the precise relationship between Hardy's test and the CHSH test? To answer this question, we found it very instructive to investigate the geometry of the sets of joint probabilities defined by the two tests.

Given a set of observables $M_1=X_1,Y_1$ and $M_2=X_2,Y_2$ with outcomes $x_j=\pm$ and $y_j=\pm(j=1,2)$, an entire correlation table of 16 joint probabilities $P(m_1,m_2|M_1,M_2)$ can be regarded as a point in the 16-dimensional vector space $\mathbb{R}^{16}$. The correlation tables cannot span the whole space $\mathbb{R}^{16}$ because of the various constraints imposed on the joint probabilities, as discussed in Sec. II A. For example, the positivity and normalization constraints, (1) and (2), define a convex subset. The causality constraints (3) restrict further the subset, and lead to a convex subset in the form of a polytope which we call the "causal polytope" $\mathcal{C}$. A polytope is the higher dimensional generalization of a polyhedron in three dimensions with flat surfaces (i.e., given by linear equations) and a finite number of vertices. For the situation considered here, there are 12 linear equations, 4 from the normalization constraints (1) and 8 from the causality constraints (3). Only 8 of them are linearly independent, and thus the causal polytope $\mathcal{C}$ is eight dimensional (8D). It has 7D facets. Correlation tables restricted additionally to Eq. (4) form also a convex polytope, $\mathcal{L}$, which is commonly called the "local polytope," or "Bell polytope." The local polytope $\mathcal{L}$ lies inside the causal polytope $\mathcal{C}$ [21–23,25]. As was shown by Fine [21], the CHSH inequalities together with the positivity constraints (2) form all the facets of $\mathcal{L}$, and give therefore a complete characterization of all LHV correlations. Quantum correlations can lie outside $\mathcal{L}$, but are always inside $\mathcal{C}$. They also form a convex set, but not in the form of a polytope. They are still restricted by Cirel'son's bound, which gives an upper bound $2\sqrt{2}$ for the left-hand side of the CHSH inequality [36].

All vertices of the polytope $\mathcal{C}$ have all joint probabilities either equal zero or one. There are 24 vertices, 16 of which

represent local correlations (called "local vertices"), and 8 represent nonlocal correlations. The vertices which represent local correlations are the vertices of the Bell polytope. They can be parametrized by four binary variables, $\alpha,\beta,\gamma,\delta \in \{0,1\}$. If we also code measurement outcomes and observables with binaries $(M_j=X_j,Y_j \mapsto 0,1$ and $m_j=\pm \mapsto 0,1$ for $j=1,2)$, they can be found from [25]

$$P(m_1,m_2|M_1,M_2) = \begin{cases} 1, & m_1=\alpha M_1 \oplus \beta \text{ and } m_2=\gamma M_2 \oplus \delta, \\ 0, & \text{otherwise}, \end{cases} \tag{16}$$

where $\oplus$ denotes addition modulo 2. Hardy's equations (5)–(8) are four more independent linear constraints, which thus restrict us to a 4D subspace of the 8D polytope $\mathcal{C}$. Indeed, the remaining joint probabilities [besides the ones chosen to be zero in Eqs. (5)–(8), can be parametrized as

$$P(+-|XX)=1-P(--|XY),$$

$$P(-+|XX)=1-P(--|YX),$$

$$P(--|XX)=-1+P(--|XY)+P(--|YX),$$

$$P(+-|XY)=1-P(--|XY)-P(-+|YY),$$

$$P(++|XY)=P(-+|YY),$$

$$P(++|YX)=1-P(--|YY)+P(-+|YY),$$

$$P(-+|YX)=-P(--|YX)+P(--|YY)+P(-+|YY),$$

$$P(+-|YY)=1-P(--|YY)-P(-+|YY). \tag{17}$$

All 16 joint probabilities are now determined once we specify $P(--|XY)$, $P(--|YX)$, $P(-+|YY)$, and $P(--|YY)$. Thus, Hardy's equations span a 4D polytope $\mathcal{H}$ which we will call "Hardy's polytope." In the following we will group the four independent joint probabilities in a 4D vector $\mathbf{p}=[P(--|XY),P(--|YX),P(-+|YY),P(--|YY)]$. It is straightforward to check that five of the 16 local vertices satisfy Eq. (17), namely those given by $\mathbf{p}=(1,0,0,0)$, $\mathbf{p}=(1,0,0,1)$, $\mathbf{p}=(1,1,0,1)$, $\mathbf{p}=(0,1,0,1)$, and $\mathbf{p}=(0,1,1,0)$. The other local vertices can be covered by another set of Hardy's equations generated from Eqs. (5)–(8) through local permutations of measurements, but in the following we will focus on one given set of Hardy's equations, i.e., on a single polytope $\mathcal{H}$. The five local vertices are the *only* vertices of $\mathcal{H}$, as can be directly verified by looking at all combinations of probabilities equal to zero or one for the elements of $\mathbf{p}$, calculating the remaining probabilities, and checking whether they fulfill normalization, positivity, and causality. Taking one of the five vertices as origin, we have four linearly independent vectors pointing to the other four vertices, which thus allow one to entirely span $\mathcal{H}$. This by itself does not mean yet that $\mathcal{H}$ lies in a facet of $\mathcal{L}$, as a polytope spanned by local vertices might lie in the interior of $\mathcal{L}$. However, we know that for all points within $\mathcal{H}$, in particular with the three probabilities in Eqs. (5)–(7) equal to zero, adding an infinitesimally small value to $P(++|YY)$ moves us outside the realm of LHV theories, by construction of Hardy's argument. Thus, for all points in $\mathcal{H}$ where a positive $P(++|YY)$ is not prohibited by other constraints (normalization and positivity of other joint probabilities) $\mathcal{H}$ must lie inside an *interface* between $\mathcal{L}$ and the remainder of $\mathcal{C}$. This interface must be a single facet of $\mathcal{L}$ or an edge, as otherwise $\mathcal{H}$ would not be convex. [For points where $P(++|YY)$ is prevented from taking positive values, $\mathcal{H}$ may lie within one of the trivial facets of $\mathcal{L}$ given by the positivity and upper bound one of all joint probabilities.] Thus, Hardy's equations define a 4D polytope contained within a 7D facet, which forms a boundary of the local polytope $\mathcal{L}$ with the set of non-local correlations, and hence corresponds to a CHSH inequality.

Suppose now that we add a small value ϵ to any of the probabilities in the first three Hardy equations, Eqs. (5)–(7), i.e., move outside of $\mathcal{H}$ in a different direction. Since we were already inside the interface between the local and the other causal correlations described by CHSH inequalities, the best we can do if we want to stay in $\mathcal{L}$ is to move within the facet. This suggests that a generalization of Hardy's equations to a necessary condition for LHV theories with finite values of the probabilities in Eqs. (5)–(7) should lead immediately to a CHSH inequality. Indeed, we will see in the following section (Sec. III D) that this is the case.

In order to visualize the polytope $\mathcal{H}$ in the subspace of the components of $\mathbf{p}$, we present in Fig. 1 several 3D cuts of $\mathcal{H}$, namely for $P(--|YY)=0,\frac{1}{4},\frac{1}{2}$, and 1. We see that for $P(--|YY)=0$ the polytope degenerates to a straight diagonal line, from $\mathbf{p}=(0,1,1,0)$ to $\mathbf{p}=(1,1,0,0)$. For finite values of $P(--|YY)$, the line widens to a cylinder with the cross section of a right-angled isosceles triangle in the planes of constant $P(-+|YY)$. These triangles move along the mentioned diagonal with increasing $P(-+|YY)$, until-they hit the boundary $P(--|XY)=0$. The length of the short sides of the triangles are given by $P(--|YY)$. Altogether, we can describe the polytope $\mathcal{H}$ by the four inequalities

$$0 \leqslant P(--|YY) \leqslant 1, \tag{18}$$

$$0 \leqslant P(-+|YY) \leqslant 1-P(--|YY), \tag{19}$$

$$1-P(-+|YY)-P(--|YY) \leqslant P(--|XY) \leqslant 1-P(-+|YY), \tag{20}$$

$$1-P(--|XY) \leqslant P(--|YX) \leqslant 1-P(--|XY)+P(--|YY). \tag{21}$$

The five local vertices which satisfy Eqs. (17) show up here as corners (1,0,0) twice, once for $P(--|YY)=0$ and once for $P(--|YY)=1$; $\mathbf{p}=(1,1,0)$ and $\mathbf{p}=(0,1,0)$ for $P(--|YY)=1$, and $\mathbf{p}=(0,1,1)$ for $P(--|YY)=0$.

A final remark is in order about the quantum states which allow to falsify LHV theories using Hardy's test. As mentioned, almost all pure states allow to demonstrate Hardy nonlocality, but the singlet state, which violates the CHSH inequality maximally, does not. How is this possible if $\mathcal{H}$ is a subset of an interface described by a CHSH inequality? The reason for this is that no set of observables X_1,Y_1,X_2,Y_2

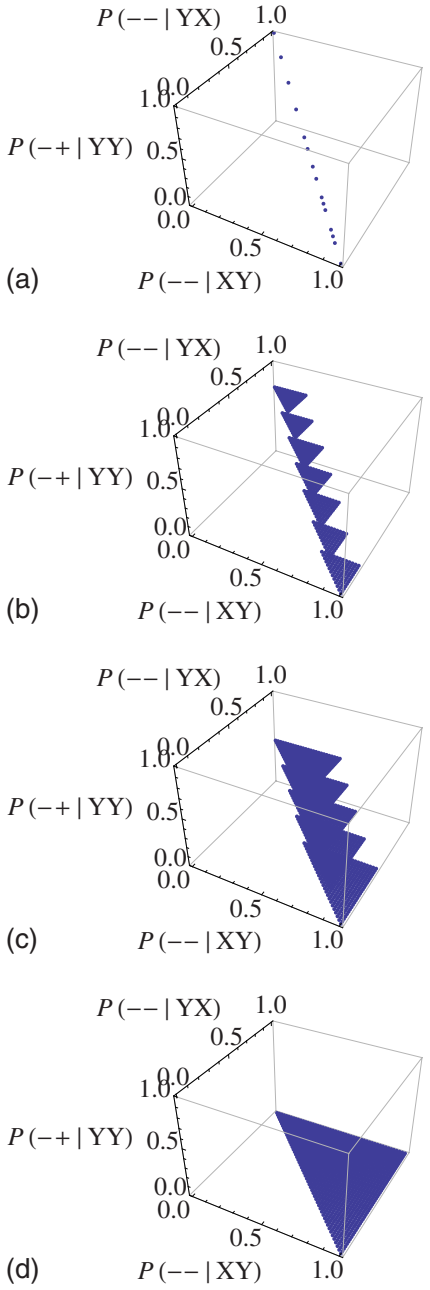

FIG. 1. (Color online) 3D cross sections of the Hardy's polytope $\mathcal{H}$ for $P(--|YY)=0$ (a), 0.25 (b), 0.5 (c), and 1 (d). All cross sections are cut once more at constant values $P(-+|YY)$ to reveal the triangular 2D cross sections.

can be found such that Eq. (8) is violated while Eqs. (5)–(7) are all satisfied. The set of correlations which satisfy Hardy's equations (5)–(7) define a 5D subset of $\mathcal{C}$, and only in this subset can Hardy's test exclude LHV theories. The singlet state leads to correlations, which, no matter the choice of observables, are outside of this subset.

D. Hardy's test in the presence of imperfections

In any realistic experimental situation, it will be difficult to fulfill Eqs. (5)–(7) *exactly*. It is therefore essential to analyze the effects of various imperfections, which may lead to finite values of the probabilities in Eqs. (5)–(7). Errors can occur in the preparation of the ideal quantum mechanical state $|\psi\rangle$, in the construction of the measurement operators X_j and Y_j, and due to detection problems, including particle loss. Suppose then that, say, $P(++|XX)$ has some finite but small value, $P(++|XX)=\epsilon_1$. Immediately the logic of Hardy's argument ceases to work, and nothing prevents an outcome $(++|YY)$. The same holds true for the other two probabilities in Eqs. (6) and (7), for which we may assume that they take on finite values $P(+-|YX)=\epsilon_2$, and $P(-+|XY)=\epsilon_3$. Furthermore, the logic of Hardy's argument also ceases to work if a particle can be lost, as this corresponds to a *third* outcome, which we will label "0" for any measurement. We should therefore also consider the situation where probabilities such as $P(+0|YX)=\epsilon_4$ and $P(0+|XY)=\epsilon_5$ can become finite. For continuity reasons it is clear that $P(++|YY)$ cannot jump immediately to arbitrarily large values if any of the ϵ_i takes on a very small but finite value. In other words, there should be a bound on $P(++|YY)$ depending on the ϵ_i. We will now show that this bound is equivalent to the CHSH inequality.

The key to generalizing Hardy's argument to finite values of the ϵ_i is replacing logical implications by set-theoretical inclusions. This approach was pioneered very recently by Ghirardi and Marinatto (GM) [26,27]. The sets in question are sets of values of hidden variables which imply certain outcomes of measurements. Following the steps in [26], only slightly generalized to different ϵ_ν and equalities instead of bounds for the joint probabilities, we immediately find the necessary condition

$$P(++|YY) \leqslant \sum_{\nu=1}^{5} \epsilon_\nu \tag{22}$$

for any LHV theory. Note that Eq. (22) is based solely on classical set-theory and does not make any assumption on how the measurement outcomes are generated. The probabilities ϵ_4 and ϵ_5 may not be measurable through a direct correlation measurement, but conservation of probability demands

$$P(+0|YX) = P^{(1)}(+|Y) - P(++|YX) - P(+-|YX) \tag{23}$$

and similarly for $P(0+|XY)$. Using this and inequality (22), we are immediately led to the CH inequality [37],

$$P(++|XY) + P(++|YX) + P(++|YY) - P(++|XX) - P^{(1)}(+|Y) - P^{(2)}(+|Y) \leqslant 0. \tag{24}$$

The CH inequality (24) is mathematically equivalent to the more familiar CHSH inequality [19] based on expectation values for dichotomic observables with measurement outcomes ± 1,

$$\langle X_1 Y_2\rangle + \langle Y_1 X_2\rangle + \langle X_1 X_2\rangle - \langle Y_1 Y_2\rangle - 2 \leqslant 0, \tag{25}$$

if particle loss is excluded [38]. This can be easily seen by using conservation of probability to express all four probabilities appearing in an expectation value such as $\langle Y_1 X_2\rangle$ in terms of the sole probability $P(++|YX)$ (and similarly for all other expectation values). Thus, the CHSH inequality can be

considered as a natural generalization of Hardy's equations—or Hardy's equations as a special case of the CHSH inequality—once the slightest imperfections need to be taken into account (see also [28]). Not withstanding the fact that Hardy's test has always been considered apart from other quantum nonlocality tests, this should come to no surprise, as in the 2222 scenario (i.e., $n_1=n_2=k_1=k_2=2$) two observables for both Alice and Bob with two possible values each, the only relevant inequality is the CHSH inequality [21–24], in the sense that if any inequality linear in the relevant joint- and single-particle probabilities is violated in this scenario, so is one of the CH inequalities constructed from Eq. (24) through symmetry operations such as particle exchange or relabeling of measurement results. Thus, as soon as Hardy's test needs to be formulated using bounds on probabilities, the resulting inequality can be at most as strong as the CHSH inequality. Note that in the experimental realization in Ref. [34] a similar inequality was derived in order to deal with imperfections.

Our derivation of the CHSH inequality as a generalized Hardy's test also sheds a new light on the former in the following sense: The inequality (24) provides a necessary condition for LHV theories even if particles can be lost. However, this does not change the status of the problem of the detector loophole. A violation of Eq. (24) would always have been considered as falsification of a LHV description, if the probabilities were the ones describing the whole ensemble of pairs used, and not just the pairs which were detected. Otherwise an additional fair sampling assumption comes in, which is the origin of the detector loophole.

E. The CHSH test with particle loss

In reality, particles can be lost without any measurement signal, on the way from the source to the detector, or due to nonideal detectors. Particle loss may be considered as a third measurement outcome, say, "0." We are therefore dealing with the case of $n_1=n_2=2$ and $k_1=k_2=3$. In such a case there exists an inequality, called I_{2233} inequality,

$$\begin{aligned} I_{2233} = {} & P(-+|YY) + P(++|YY) + P(--|YY) + P(++|XY) \\ & + P(--|XY) + P(+-|XY) + P(++|YX) + P(--|YX) \\ & + P(+-|YX) - P(++|XX) - P(--|XX) - P(+-|XX) \\ & - P^{(1)}(-|Y) - P^{(1)}(+|Y) - P^{(2)}(+|Y) - P^{(2)}(-|Y) \leqslant 0, \end{aligned} \tag{26}$$

which is more relevant than the CHSH inequality [39,40]. In other words, it can detect quantum nonlocal correlations, even if the CHSH inequality fails to do so. It appears therefore to be worthwhile examining, whether experiments which include the possibility of particle loss would not better test for nonlocality using the I_{2233} inequality. It is the purpose of the present section to show that this is not the case.

Interestingly, the inequality is maximally violated by a nonmaximally entangled state, if the three outcomes correspond to actual quantum states [41]. However, in the case of particle loss as third outcome, the events are not independent. If we assume that an electron is lost with probability r on Alice's side, and with the same probability (and independently) on Bob's side, I_{2233} becomes

$$\begin{aligned} I_{2233}(r) = {} & [P(-+|YY) + P(++|YY) + P(--|YY) \\ & + P(++|XY) + P(--|XY) + P(+-|XY) \\ & + P(++|YX) + P(--|YX) + P(+-|YX) \\ & - P(++|XX) - P(--|XX) - P(+-|XX)](1-r)^2 \\ & - [P^{(1)}(-|Y) + P^{(1)}(+|Y) + P^{(2)}(+|Y) + P^{(2)}(-|Y)] \\ & \times (1-r) \leqslant 0. \end{aligned} \tag{27}$$

Whereas in Eq. (26) the probabilities mean the actually observed ones, the probabilities in Eq. (27) are the ideal probabilities without particle loss. The latter permit only two values for each observable, and we have conservation of these ideal probabilities, such as

$$P^{(1)}(+|X) = P(++|XX) + P(+-|XX) \tag{28}$$

This allows one to rewrite $I_{2233}(r)$ as

$$I_{2233}(r) = I_{CHSH}(r) - r(1-r)[P^{(1)}(+|X) + P^{(2)}(+|X)] \leqslant 0, \tag{29}$$

where

$$\begin{aligned} I_{CHSH}(r) = {} & [P(++|YY) + P(++|XY) + P(++|YX) \\ & - P(++|XX)](1-r)^2 - [P^{(1)}(+|Y) + P^{(2)}(+|Y)] \\ & \times (1-r) \leqslant 0 \end{aligned} \tag{30}$$

is the CHSH inequality modified for the possibility of particle loss (see also Sec. III D below). For $r=0$ we have $I_{2233}(0)=I_{CHSH}(0)=I_{CHSH}$, as it should be. Due to the positivity of the term $P^{(1)}(+|X)+P^{(2)}(+|X)$ in Eq. (29), we have $I_{2233}(r)\leqslant I_{CHSH}(r)$, i.e., if $I_{2233}(r)\leqslant 0$ is violated, so is $I_{CHSH}(r)\leqslant 0$, but not necessarily the other way round. Thus, we have established that if the third measurement outcome is particle loss, the CHSH inequality is more relevant than the I_{2233} inequality, contrary to the case of genuine three-outcome measurements.

To summarize, we have established the CH inequality (24) or, equivalently, the CHSH inequality (25) as the relevant inequality for all three tests considered above: ideal Hardy's test, Hardy's test with imperfections, and the CHSH test including particle loss. This leaves open the question, however, which test will be violated in a more robust way in an experiment. Optimizing different tests leads indeed to *different* experiments, i.e., not only the state to be constructed is different, but so are the corresponding measurement operators. Since all tests will be based on the CHSH inequality, we will distinguish different tests by the specific experimental situations. Under the "CHSH test" we understand an experiment using the singlet state (or, in the case of noise, a state close to the singlet) in order to show a violation of the CHSH inequality. We will call "Hardy's test" an experiment using a state close to the ideal Hardy state (15) in order to show a violation of the CHSH inequality (see Sec. II D above). Experimentally, it is desirable to obtain as strong a violation as possible, but also in a range of parameters as wide as possible. Since the CHSH inequality is known to be violated

maximally for a singlet state [36], the CHSH test wins in the first category. However, the second category is important in the case of uncontrolled fluctuations of parameters in the experiment, and the question which test fares best in this category is *a priori* open. It is best answered for a specific experimental setup, and this is what we are going to discuss now.

III. PROPOSED EXPERIMENTAL SETUP

We propose a flexible mesoscopic circuit which allows to perform Hardy's test and the CHSH test discussed in the previous section, and compare then the expected parameter regions in which these tests are expected to fail according to quantum mechanics. Spacelike separation of measurements is unlikely to be achieved on a chip in the near future, where the measurement stations are separated by a few μm. However, the locality condition is known to be a special case of the more general concept of noncontextuality [42]. Noncontextuality in quantum mechanics (QM) means that the measurement of an observable A does not influence the outcome of the measurement of another observable B that commutes with A. The theories ruled out by a successful experiment with a mesoscopic circuit should therefore be classified as "noncontextual hidden variable theories" (NCHV). While a local hidden variable (LHV) theory might still explain the results, it would have to introduce so far unknown interactions. Replacing the belief in locality by the more general *assumption* of noncontextuality is indeed natural once one starts to doubt the validity of locality in quantum mechanics (see [43–46] for recent attempts to explain the quantum world with nonlocal realistic theories). The conclusions drawn from a NCHV theory in terms of bounds on correlations are exactly the same as for a LHV theory—only the physical origin of the assumed independence of Alice's measurement results on Bob's settings is different. The violation of any of the noncontextuality conditions discussed below may be viewed as signature of true quantum correlations in a mesoscopic circuit.

A. Mesoscopic circuit

The circuit consists of two coupled electronic Mach-Zehnder (MZ) interferometers fabricated on a quantum Hall bar [13,47,48], see Fig. 2(a). One of the two MZ interferometers is formed of the outer edge channel of the quantum Hall liquid with filling factor 2, whereas the other uses the inner channel. The electronic beam splitters (BS) in the MZ interferometers are realized by quantum point contacts (QPC). A QPC can be fine tuned so as either to block the inner channel completely and partially transmit the outer channel, or to entirely transmit the outer channel and partially reflect the inner channel. In this way a QPC can operate as a BS selectively on one of the two edge channels. In order to create an entangled state, the two MZ interferometers should be coupled. The coupling in our scheme arises from the Coulomb repulsion between the electrons in the two parallel edge channels. The repulsive potential affects the phases of the interacting electrons, and thus the coupling provides a controlled phase shift between the two MZ interferometers. This has been recently demonstrated experimentally [48]. As we will explain below, the chip should be fed with synchronized single-electron sources rather than through more common contact reservoirs, which inject continuous streams of electrons. Among several possible methods, we propose the use of the coherent single-electron source based on a coherent capacitor. Demonstrated in a recent experiments [49], this source allows well-controlled injection times, well-defined energy of the injected electrons, as well as good control of the input current through the frequency of the pump (about 180 MHz in Ref. [49]).

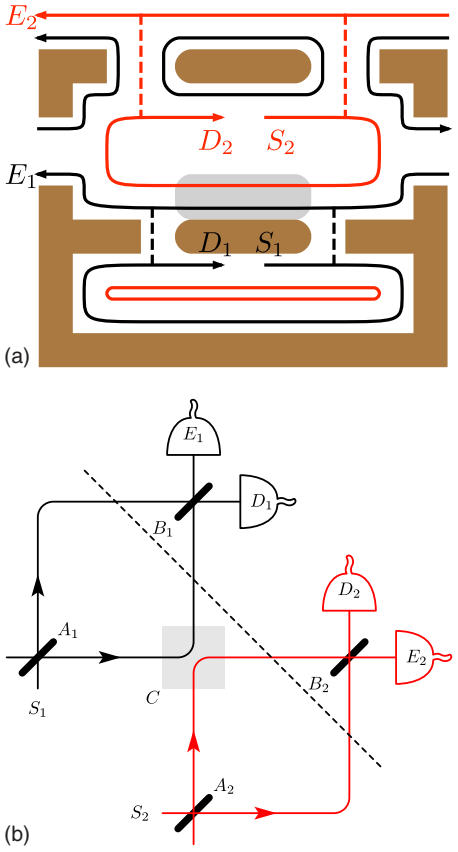

FIG. 2. (Color online) (a) A schematic of the mesoscopic circuit with two coupled Mach-Zehnder interferometers fabricated on a quantum Hall bar and (b) its equivalent diagram. The arrowed (black and red) lines are the edge channels of the quantum Hall liquid with filling factor 2. S_j $(j=1,2)$ denote the electron sources, A_j and B_j the beam splitters (quantum point contacts), D_j and E_j the electron detectors, and C the conditional phase shift. The coupling is realized by the Coulomb interaction between the two channels in the gray shaded region in (a).

Let us denote by S_j $(j=1,2)$ the input port through which electrons are injected to the jth MZ interferometer, by A_j and B_j, the two beam splitters, and by D_j and E_j, the two output ports where the electrons are detected; see Fig. 2(b). We attribute the value +1 to detection in D_j (basis state $|0\rangle$), and −1 to detection in E_j (basis state $|1\rangle$). Using the fact that only relative phases between the two branches in an MZ interferometer are relevant, we may represent the beam splitters by a real orthogonal matrix of the form

$$U_B(\theta) = \begin{pmatrix} \cos\theta & -\sin\theta \\ \sin\theta & \cos\theta \end{pmatrix} \tag{31}$$

in the basis $\{|0\rangle,|1\rangle\}$. Phase shifts within a MZ interferometer are described by

$$U_P(\phi) = \begin{pmatrix} 1 & 0 \\ 0 & e^{i\phi} \end{pmatrix}. \tag{32}$$

The coupling C reads

$$U_C(\phi) = \begin{pmatrix} 1 & & & \\ & 1 & & \\ & & 1 & \\ & & & e^{i2\phi} \end{pmatrix} \tag{33}$$

in the basis $\{|00\rangle,|01\rangle,|10\rangle,|11\rangle\}$ with $|\sigma_1\sigma_2\rangle \equiv |\sigma_1\rangle \otimes |\sigma_2\rangle$. A_1, A_2 and C are used for the preparation of the entangled state, while B_1 and B_2 allow to select the four different quantum measurements. The two interacting MZ interferometers realize the unitary transformation

$$U = [U_B(\theta_1') \otimes U_B(\theta_2')][U_P(\phi_1) \otimes U_P(\phi_2)]U_C(\phi) \times [U_B(\theta_1) \otimes U_B(\theta_2)]. \tag{34}$$

Even though there have been experimental demonstrations of high precision single-electron detection [50–53], none of them is fast enough for nanosecond time scales. Therefore, we propose to use low-frequency current cross correlations instead [5,7,12,54]. The zero-frequency spectral density $S_{M_1M_2}(H_1,H_2)$ of the correlations between two drains H_1,H_2 (where $H_j \in \{D_j,E_j\}$, $j=1,2$) of the current fluctuations $\delta I_j(H_j)=I_j(H_j)-\langle I_j(H_j)\rangle$ is defined as

$$S_{M_1M_2}(H_1,H_2) = \int_{-\infty}^{\infty} dt \langle \delta I_1(H_1,t)\delta I_2(H_2,0)\rangle. \tag{35}$$

To simplify notation, we have suppressed the dependence of δI_j on the measurement settings, coded in the subscripts of $S_{M_1M_2}(H_1,H_2)$ ($M_j=X_j$ or Y_j). If the electron pairs from the synchronized sources S_1 and S_2 are well separated in each interferometer (at 180 MHz operation the temporal width of the electron wave package was below 1 ns for optimal current quantization in [49]), $S_{M_1M_2}(H_1,H_2)$ is directly related to the joint probabilities of Eqs. (5)–(8) [7,12]. For example, we have

$$P(+-|YX) = \frac{2\pi}{eI_0} S_{YX}(D_1,E_2), \tag{36}$$

and correspondingly for the other joint probabilities in Eqs. (5)–(8), where I_0 is the injection current from the single-electron sources S_1 and S_2 ($\approx$5 pA in [49]). The requirement for well separated electrons for the validity of Eq. (36) and the need for well-defined interaction phases (and thus simultaneous arrival of the electrons in the interaction area C), motivate the use of synchronized single electron sources. As a byproduct, the production rate of electron pairs is precisely known. This is important for a convincing falsification of any NCHV model, as discussed in Sec. I at the beginning. As Eq. (36) makes obvious, the joint probabilities for our setup are normalized relative to the absolute pump rates I_0, and this allows us to avoid the description by an NCHV model as in Ref. [15].

B. Parameters for Hardy's test

For Hardy's test, one should create the state (15). In principle two full MZ interferometers and thus four BSs are necessary to do so. For the choice of measurement operators, one would need two more BSs (one for Alice, one for Bob). However, since these BSs just perform local unitary rotations, we can combine the last two BSs on each side, and therefore perform all experiments for the correlations (5)–(8) with just two BSs per party. We put the beam splitter A_1 into a fixed mode associated with the unitary matrix $V_1 = U_B(\pi/4)$, create $V_2=U_B(\theta_0)$ with A_2, and adjust the coupling to $V_0=U_C(\phi_0)$, where the optimal values θ_0 and ϕ_0 are given by

$$\cos(2\theta_0) = \cos(2\phi_0) = 2-\sqrt{5}. \tag{37}$$

This leads to the entangled state $|\psi\rangle = V_0(V_1 \otimes V_2)|00\rangle$,

$$|\psi\rangle = \frac{\cos\theta_0}{\sqrt{2}}(|00\rangle + |10\rangle) + \frac{\sin\theta_0}{\sqrt{2}}(|01\rangle + e^{i2\phi_0}|11\rangle), \tag{38}$$

achieved after the electrons pass through A_1, A_2, and undergo the conditional phase shift C.

Following the lines of Refs. [18,26,27,55] we implement the measurements X_1 and Y_1 by switching the beam splitter B_1 between the two modes associated with the unitary matrices $U_1=U_B(\pi/4)$ and $W_1=U_P(2\phi_0)U_B(\pi/4)U_P(-2\phi_0)$, and the beam splitter B_2 between the two modes $U_2=U_B(0)$ and $W_2=U_P(\phi_0)U_B(\chi)U_P(-\phi_0)$, where $\cot\chi=\tan\theta_0\cos\phi_0$. In other words, the measurements X_j and Y_j are given by $X_j=U_j^\dagger Z U_j$ and $Y_j=W_j^\dagger Z W_j$, respectively, where $Z=|0\rangle\langle 0| - |1\rangle\langle 1|$. The last phase shifts in W_1 and W_2 change the phases of the computational basis states immediately before detection and do not modify the final probabilities. Omitting them brings the total unitary transformation to the form (34) with seven parameters, whose optimal values we have summarized in Table I. It is then straightforward to see that the quantum mechanical joint probabilities P_ψ associated with the state $|\psi\rangle$ in Eq. (38) verify Eqs. (5)–(7), whereas instead of Eq. (8) we have Eq. (14), i.e., a violation of the inequality in about 9% of all cases.

C. Parameters for CHSH test

The singlet state can be created as

$$|\psi_s\rangle = \left[U_B\left(\frac{\pi}{4}\right) \otimes U_B(0)\right] U_{CP}\left(\frac{\pi}{2}\right) \left[U_B\left(\frac{\pi}{4}\right) \otimes U_B\left(\frac{\pi}{4}\right)\right] \times |00\rangle. \tag{39}$$

The optimal choice of measurements for a maximal violation of Eq. (24) is

TABLE I. Optimal parameters for all four measurements for Hardy's test and the CHSH test; $\theta_0=\phi_0=[\arccos(2-\sqrt{5})]/2$, $\chi=\operatorname{arccot}(\tan\theta_0\cos\phi_0)$.

	M_1,M_2	θ_1^{opt}	θ_2^{opt}	ϕ^{opt}	ϕ_1^{opt}	ϕ_2^{opt}	$\theta_1'^{opt}$	$\theta_2'^{opt}$
Hardy	X,X	$\pi/4$	θ_0	ϕ_0	0	0	$\pi/4$	0
Hardy	X,Y	$\pi/4$	θ_0	ϕ_0	0	$-\phi_0$	$\pi/4$	χ
Hardy	Y,X	$\pi/4$	θ_0	ϕ_0	$-2\phi_0$	0	$\pi/4$	0
Hardy	Y,Y	$\pi/4$	θ_0	ϕ_0	$-2\phi_0$	$-\phi_0$	$\pi/4$	χ
CHSH	X,X	$\pi/4$	$\pi/4$	$\pi/2$	0	π	$\pi/4$	$\pi/8$
CHSH	X,Y	$\pi/4$	$\pi/4$	$\pi/2$	0	π	$\pi/4$	$3\pi/8$
CHSH	Y,X	$\pi/4$	$\pi/4$	$\pi/2$	0	π	0	$\pi/8$
CHSH	Y,Y	$\pi/4$	$\pi/4$	$\pi/2$	0	π	0	$3\pi/8$

$$X_1=\sigma_z,$$

$$Y_1=\sigma_x,$$

$$X_2=\frac{1}{\sqrt{2}}(\sigma_z-\sigma_x),$$

$$Y_2=-\frac{1}{\sqrt{2}}(\sigma_x+\sigma_z), \tag{40}$$

where σ_x and σ_z are Pauli matrices. This implies that the BS B_1 should be set to full transmission ($U_B(0)$) for $M_1=X_1$, and to $U_B(-\frac{\pi}{4})$ for $M_1=Y_1$, as $X_1=U_B(\frac{\pi}{4})ZU_B(-\frac{\pi}{4})$. For B_2 we choose angles $\frac{\pi}{8}$ or $\frac{3\pi}{8}$ for X_2 or Y_2, respectively, as $X_2=U_B(-\frac{\pi}{8})ZU_B(\frac{\pi}{8})$ and $Y_2=U_B(-\frac{3\pi}{8})ZU_B(\frac{3\pi}{8})$. In Table I we summarize the parameters for the different BSs and phase shifters for all four measurements for Hardy's test and the CHSH test.

D. Imperfections

Let us now calculate, both for Hardy's test and the CHSH test, the range of fluctuations of the seven angles θ_j, θ_j', ϕ_j, $(j=1,2)$, and ϕ of the unitary matrix U in Eq. (34) around their optimal values (see Table I), for which QM still predicts a violation of Eq. (24). Fluctuations in these angles lead to mixed states ρ at the output ports, which depend on the test and the measurements. We denote the quantum mechanical predictions of the probabilities corresponding to ρ by P_ρ. The final QM joint probabilities in Eq. (24) are given by postprocessing the P_ρ with a classical stochastic map that models particle loss. Besides electrons going undetected, an electron may also be detected in the wrong output port (E_j instead of D_j, or vice versa), or an electron might be detected erroneously in both output ports. The last process, witnessed by a finite value of the correlator $S_{M_1M_2}(E_j,D_j)$, should be taken care of experimentally by subtracting the dark count. Detecting an electron in the wrong drain can be shown to be equivalent to a bit flip error after the state preparation and can be included in the fluctuations of the 7 angles. As we exclude joint dark counts, the final predictions for the joint probabilities in Eq. (24) are then simply obtained by multiplying the P_ρ with a factor $(1-r)^2$, where r is the single electron loss rate per interferometer, indicating that no electron was lost, neither on Alice's nor Bob's side. The single particle probabilities are multiplied only with a factor $(1-r)$. This leads to inequality (30). Note that r can be measured through $\langle I(D_j)\rangle+\langle I(E_j)\rangle=I_0(1-r)$ for known I_0; see the discussions in Sec. II E.

We have estimated the allowed range of errors for uniform distributions of the relevant fluctuations, independent of the measurement chosen. Note that different probabilities correspond to different settings of the BS, and thus to a different final state before the application of the measurement operator Z, even without fluctuations. Correspondingly, also a different final mixed state is produced for each different joint probability function. This can be considered as the Schrödinger picture of the measurement process (same operator, different states) in contrast to the more familiar Heisenberg picture (fixed state, different measurements). Since the CHSH inequality (24) is linear in the probabilities, we may as well average the probabilities themselves over the distributed parameters. For example, when the first beam splitters A_1 and A_2 are subject to errors in the tuning of the transmissions, the allowed error range is given by the condition

$$\frac{1}{4\delta_1\delta_2}\int_{\theta_1^{\rm opt}-\delta_1}^{\theta_1^{\rm opt}+\delta_1}d\theta_1\int_{\theta_2^{\rm opt}-\delta_2}^{\theta_2^{\rm opt}+\delta_2}d\theta_2\{[P_\psi(++|XX)+P_\psi(++|XY)+P_\psi(++|YX)-P_\psi(++|YY)](1-r)-P_\psi^{(1)}(+|Y)-P_\psi^{(2)}(+|Y)\}\leqslant 0, \tag{41}$$

where $\theta_j^{\rm opt}$ $(j=1,2)$ are the optimal settings for the corresponding test and measurements (different for different terms in the integral, see Table I). In the above inequality (41), $P_\psi(m_1,m_2|M_1,M_2)$ denote the quantum mechanical probabilities corresponding to the states $|\psi(\theta_1,\ldots,\theta_2')\rangle=U(\theta_1,\ldots,\theta_2')|00\rangle$ with U from Eq. (34). As such, the θ_j dependence of $P_\psi(m_1,m_2|M_1,M_2)$ is through the state $|\psi(\theta_1,\cdots,\theta_2')\rangle$. Note that the marginal probability $P_\psi^{(1)}(+|Y)$ is implemented experimentally either by $P_\psi^{(1)}=P_\psi(++|YY)+P_\psi(+-|YY)$ or by $P_\psi^{(1)}=P_\psi(++|YX)+P_\psi(+-|YX)$, and similarly for $P_\psi^{(2)}(+|Y)$.

Figure 3 shows that for Hardy's test all angles can fluctuate over intervals of the order of 1 radian, if no electron is lost, whereas for small fluctuations of the angles loss rates up to 15% in each interferometer can be tolerated, in agreement with earlier findings about the detector efficiency needed to avoid a detector loophole for Hardy nonlocality [56]. However, for the CHSH test the allowed range of fluctuations is even larger (see Fig. 3). Altogether, we see that our mesoscopic scheme is very robust against possible imperfections. The scheme might therefore be sufficiently robust for experimental implementation with present day technology.

IV. CONCLUSIONS

We have compared three different tests of quantum nonlocality, both on a theoretical level, and with respect to a possible implementation in a mesoscopic circuit. We have shown that Hardy's test becomes a special instance of the more general CHSH inequality as soon as imperfections have to be taken into account. We have uncovered the deeper geometrical reason for this fact by establishing that Hardy's equations describe a 4D convex polytope embedded inside the interface, described by a CHSH inequality, between the polytope of local correlations and the remaining causal correlations. We have also demonstrated that the inequality I_{2233}, relevant for experiments with three outcomes per observable, is superseded by the CHSH inequality if the third measurement outcome is particle loss. We have proposed a flexible measurement setup based on two interacting Mach-Zehnder interferometers formed from Hall-bar edge states at filling factor 2 and quantum point contacts, which allows to implement both Hardy's test and the CHSH test. Based on that setup, we have shown that both Hardy's test and the CHSH test should be sufficiently robust with respect to parameter fluctuations to allow falsification of a noncontextual hidden variable description of the experiment. For the CHSH test the tolerance with respect to fluctuations of the relevant experimental parameters is substantially larger than for Hardy's test.

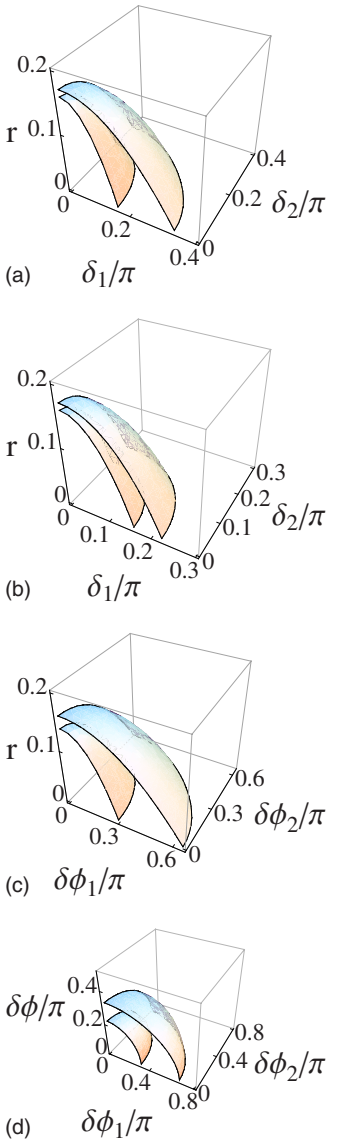

FIG. 3. (Color online) Boundaries of the regions where NCHV theories are expected to be falsified in Hardy's test (lower surfaces) and the CHSH test (upper surfaces) for a selection of different errors. (a) Allowed fluctuations δ_1 and δ_2 in θ_1 and θ_2 of the beam splitters A_1 and A_2, respectively, when electrons are lost with probability r per interferometer. (b) The same as (a) for the beam splitters B_1 and B_2. (c) The same as (a), but for the phase fluctuations $\delta\phi_1$ and $\delta\phi_2$ in the two Mach-Zehnder interferometers. (d) Same as (c), but with a phase fluctuation $\delta\phi$ in the controlled phase shift $U_C(\phi)$ instead of r for $r=0$.

ACKNOWLEDGMENTS

D.B. would like to thank Hélène Bouchiat, Izhar Neder, and Bertrand Reulet for interesting discussions. This work was supported in part by the Agence National de la Recherche (ANR), project INFOSYSQQ, Contract No. ANR-05-JCJC-0072, and the EC IST-FET project EUROSQIP. M.-S.C. was supported by the SRC/ERC program (Contract No. R11-2000-071), the KRF Grants No. KRF-2005-070-C00055 and No. KRF-2006-312-C00543, the BK21 project, and the KIAS.

[1] A. Einstein, B. Podolsky, and N. Rosen, Phys. Rev. **47**, 777 (1935).
[2] J. S. Bell, Physics (Long Island City, N.Y.) **1**, 195 (1964).
[3] A. Aspect, J. Dalibard, and G. Roger, Phys. Rev. Lett. **49**, 1804 (1982).
[4] A. Aspect, Nature (London) **398**, 189 (1999).
[5] C. W. J. Beenakker, C. Emary, M. Kindermann, and J. L. van Velsen, Phys. Rev. Lett. **91**, 147901 (2003).
[6] C. W. J. Beenakker, M. Kindermann, C. M. Marcus, and A. Yacoby, in *Fundamental Problems of Mesoscopic Physics*, edited by I. V. Lerner, B. L. Altshuler, and Y. Gefen, NATO Science Series II Vol. 154 (Kluwer, Dordrecht, 2004).
[7] P. Samuelsson, E. V. Sukhorukov, and M. Büttiker, Phys. Rev. Lett. **92**, 026805 (2004).
[8] A. V. Lebedev, G. Blatter, C. W. J. Beenakker, and G. B. Lesovik, Phys. Rev. B **69**, 235312 (2004).
[9] A. V. Lebedev, G. B. Lesovik, and G. Blatter, Phys. Rev. B **71**, 045306 (2005).
[10] A. DiLorenzo and Y. V. Nazarov, Phys. Rev. Lett. **94**, 210601 (2005).
[11] K. Kang and K. H. Lee, e-print arXiv:0707.1170.
[12] P. Samuelsson, E. V. Sukhorukov, and M. Büttiker, Phys. Rev. Lett. **91**, 157002 (2003).
[13] I. Neder, N. Ofek, Y. Chung, M. Heiblum, D. Mahalu, and V. Umansky, Nature (London) **448**, 333 (2007).
[14] M. Ansmann *et al.*, Bull. Am. Phys. Soc. **52**, L33.00005 (2007).
[15] E. Santos, Phys. Rev. A **46**, 3646 (1992).
[16] D. N. Matsukevich, P. Maunz, D. L. Moehring, S. Olmschenk, and C. Monroe, Phys. Rev. Lett. **100**, 150404 (2008).
[17] L. Hardy, Phys. Rev. Lett. **68**, 2981 (1992).
[18] L. Hardy, Phys. Rev. Lett. **71**, 1665 (1993).
[19] J. F. Clauser, M. A. Horne, A. Shimony, and R. A. Holt, Phys. Rev. Lett. **23**, 880 (1969).
[20] N. D. Mermin, Ann. N.Y. Acad. Sci. **755**, 616 (1995).
[21] A. Fine, Phys. Rev. Lett. **48**, 291 (1982).
[22] A. Fine, J. Math. Phys. **23**, 1306 (1982).
[23] R. F. Werner and M. M. Wolf, e-print arXiv:quant-ph/0107093v2.
[24] D. Collins and N. Gisin, J. Phys. A **37**, 1775 (2004).
[25] J. Barrett, N. Linden, S. Massar, S. Pironio, S. Popescu, and D. Roberts, Phys. Rev. A **71**, 022101 (2005).
[26] G. C. Ghirardi and L. Marinatto, Phys. Rev. A **73**, 032102 (2006).
[27] G. C. Ghirardi and L. Marinatto, Phys. Rev. A **74**, 062107 (2006).
[28] G. Ghirardi and L. Marinatto, Phys. Lett. A **372**, 1982 (2008).
[29] J. S. Bell, Rev. Mod. Phys. **38**, 447 (1966).
[30] L. Hardy, Phys. Rev. Lett. **71**, 1665 (1993).
[31] S. Goldstein, Phys. Rev. Lett. **72**, 1951 (1994).
[32] G. Ghirardi and L. Marinatto, Phys. Rev. A **72**, 014105 (2005).
[33] D. M. Greenberger, M. A. Horne, and A. Zeilinger, in *Bell's Theorem, Quantum Theory, and Conceptions of the Universe*, edited by E. M. Kafatos (Kluwer, Dordrecht, 1989).
[34] W. T. M. Irvine, J. F. Hodelin, C. Simon, and D. Bouwmeester, Phys. Rev. Lett. **95**, 030401 (2005).
[35] G. Di Giuseppe, F. De Martini, and D. Boschi, Phys. Rev. A **56**, 176 (1997).
[36] B. S. Cirel'son, Lett. Math. Phys. **4**, 93 (1980).
[37] J. F. Clauser and M. A. Horne, Phys. Rev. D **10**, 526 (1974).
[38] M. A. Nielsen and I. L. Chuang, *Quantum Computation and Quantum Information* (Cambridge University Press, Cambridge, 2000).
[39] D. Collins, N. Gisin, N. Linden, S. Massar, and S. Popescu, Phys. Rev. Lett. **88**, 040404 (2002).
[40] D. Kaszlikowski, L. C. Kwek, J.-L. Chen, M. Zukowski, and C. H. Oh, Phys. Rev. A **65**, 032118 (2002).
[41] A. Acín, T. Durt, N. Gisin, and J. I. Latorre, Phys. Rev. A **65**, 052325 (2002).
[42] N. D. Mermin, Rev. Mod. Phys. **65**, 803 (1993).
[43] A. J. Leggett, Found. Phys. **33**, 880 (2003).
[44] S. Gröblacher, T. Paterek, R. Kaltenbaek, Časlav Brukner, M. Zukowski, M. Aspelmeyer, and A. Zeilinger, Nature (London) **446**, 871 (2007).
[45] C. Branciard, A. Ling, N. Gisin, C. Kurtsiefer, A. Lamas-Linares, and V. Scarani, Phys. Rev. Lett. **99**, 210407 (2007).
[46] T. Paterek, A. Fedrizzi, S. Groblacher, T. Jennewein, M. Zukowski, M. Aspelmeyer, and A. Zeilinger, Phys. Rev. Lett. **99**, 210406 (2007).
[47] Y. Ji, Y. Chung, D. Sprinzak, M. Heiblum, D. Mahalu, and H. Shtrikman, Nature (London) **422**, 415 (2003).
[48] I. Neder, M. Heiblum, Y. Levinson, D. Mahalu, and V. Umansky, Phys. Rev. Lett. **96**, 016804 (2006).
[49] G. Feve, A. Mahe, J.-M. Berroir, T. Kontos, B. Placais, D. C. Glattli, A. Cavanna, B. Etienne, and Y. Jin, Science **316**, 1169 (2007).
[50] J. Bylander, T. Duty, and P. Delsing, Nature (London) **434**, 361 (2005).
[51] R. J. Schoelkopf, P. Wahlgren, A. A. Kozhevnikov, P. Delsing, and D. E. Prober, Science **280**, 1238 (1998).
[52] S. Gustavsson, R. Leturcq, T. Ihn, K. Ensslin, D. C. Driscoll, and A. C. Gossard, Physica E (Amsterdam) **40**, 103 (2007).
[53] T. Fujisawa, T. Hayashi, R. Tomita, and Y. Hirayama, Science **312**, 1634 (2006).
[54] N. M. Chtchelkatchev, G. Blatter, G. B. Lesovik, and T. Martin, Phys. Rev. B **66**, 161320(R) (2002).
[55] S. Goldstein, Phys. Rev. Lett. **72**, 1951 (1994).
[56] W. Y. Hwang, I. G. Koh, and Y. D. Han, Phys. Lett. A **212**, 309 (1996).